Dielectric Spectroscopy Analysis Using Viscoelasticity-inspired Relaxation Theory with Finite Element Modeling

He Zhao, Yang Li, L. Catherine Brinson
Department of Mechanical Engineering
Northwestern University
2145 Sheridan Road
Evanston, IL 60208, USA

Yanhui Huang, Timothy M. Krentz, Linda S. Schadler
Department of Materials Science and Engineering
Rensselaer Polytechnic Institute
110 8th Street,
Troy, NY 12180, USA

Michael Bell and **Brian Benicewicz**
Department of Chemistry and Biochemistry
University of South Carolina
631 Sumter St
Columbia, SC 29208, USA

ABSTRACT

We demonstrate the formulation of frequency-dependent dielectric permittivity by superposition of Debye functions inspired by viscoelastic relaxation theory. With multiple relaxation times and permittivity strength, a viscoelastic Prony Series is adapted to construct an expression of dielectric permittivity for polymer dielectric materials, which can be successfully matched with experimental data. We then develop a finite element modeling approach with explicit microstructure dispersion and inclusion of filler-matrix interphase using functionalized silica-epoxy nanocomposite samples as a testbed. The interphase relaxation behavior is expressed using the bulk polymer properties modified by frequency and magnitude shift factors that adjust the shape of the simulated dielectric spectrum to mimic changes in relaxation time due to the polymer/filler interaction. Finally, the influence of interphase thickness and dispersion state is investigated with parametric studies. It is found that total interphase area in the composite has a critical influence over the composite property, and by varying interphase layer and dispersion within a reasonable range, as much as 20% difference can be obtained in the simulated composite property. Our simulation results provide insights into the underlying relaxation mechanism in the interfacial region.

Index Terms — **Dielectric spectroscopy, interphase, nanocomposites, finite element modeling**

1 INTRODUCTION

DIELECTRIC polymer nanocomposites (or "nanodielectrics") have been widely studied as promising candidates for devices in electrical energy storage or high voltage electrical transmission as they combine the advantages of the high breakdown strength of the polymer matrix and/or the high or low dielectric constant of inorganic fillers [1]. Dielectric spectroscopy measures the frequency-dependent dielectric constant and dielectric loss (or tan δ). A lag in the polarization of the material due to dipole orientation or space charge displacement behind the oscillating field creates a phase lag. This is known as the dielectric relaxation, and is particularly interesting for materials operating over a wide frequency range. Unlike their microcomposite counterparts, nanodielectrics possess a large volume fraction of the filler-matrix interphase that dominates the overall behavior in the composite [2, 3]. Previous works have demonstrated that filler-

Manuscript received on 19 January 2017, accepted 9 August 2017.
Corresponding author: L.C. Brinson.

DOI: 10.1109/TDEI.2017.006563

matrix interactions can either enhance or restrict the mobility of polymer chains, and thus lead to significant changes in dielectric loss [4-6]. Recent research efforts have focused on tuning the filler surface modification to control filler dispersion as well as desired dielectric relaxation behavior [7, 8]. An accurate methodology to describe the dielectric relaxation behavior is of great value in order to provide guidelines for design of nanodielectrics.

A variety of analytical model functions have been developed to analyze the dielectric constant and spectroscopy in dielectric materials. Previous analytical studies on dielectric constants in composites rely on homogenization methods with mixing rules. Some of the broadly used models are the Maxwell-Garnett model [9], Bruggeman model [10], Lichtenecker model [11] and Hashin-Strikman model [12] for two phase systems. More recent models also account for the impact of the interfacial region, including the Todd-Shi model [13] and Vo-Shi model [14]. These models are developed from mean field approximation and can often provide qualitative prediction of effective dielectric constant in composite dielectric materials. However, these models are insufficient to capture the overall dielectric response in nanodielectric materials because they do not adequately address and explain the physics behind the impact of the filler surface chemistry on the composite response or the impact of nanofiller dispersion on bulk composite properties [7].

In terms of dielectric relaxation behavior, previous parametric model functions have been developed using the well-known standard Debye function to analyze realistic relaxation in the frequency domain. A comprehensive review of different models, including Cole-Cole, Cole-Davidson, and Havriliak-Negami, can be found in [15]. Peak broadening and skewing factors have been used to mathematically fit non-Debye relaxations that are commonly found in nanodielectrics. Although these model functions can provide accurate descriptions of the spectroscopy, none of the power law coefficients in these models have a clear physical meaning that can be correlated with the underlying physics behind phase interactions in nanodielectrics. A comprehensive parametric model able to describe dielectric relaxation behavior with clear physical meaning is still lacking.

Finite element (FE) analysis has been demonstrated as a powerful simulation tool to analyze and predict material properties in nanocomposite materials. Unlike homogenization models, FE simulation can start directly from explicit composite morphology through microscopic image analysis to provide quantitative property predictions with explicit configuration of all relevant material phases, including the interphase. This advantage makes FE a good option in the analysis of nanocomposites with dispersed fillers. Previous work on viscoelastic properties in polymer nanocomposites have demonstrated the ability of FE model to include detailed nanoparticle dispersion and agglomeration as well as the interphase region with explicitly defined material properties [16, 17]. Additionally, the storage and loss moduli of a viscoelastic material can be well analyzed by a Prony Series with parametric expression of multiple relaxation times for analysis of dynamic mechanical response [18]. The filler-matrix interphase properties in viscoelastic nanocomposites can also be described with a shift factor applied to the pure polymer properties which accounts for the altered chain mobility [19]. Recent work also includes models that take account of overlapped interphase in nanodielctrics [20]. Such approaches provide the inspiration for a more rigorous and comprehensive model for dielectric spectroscopy analysis.

In this work, we present an FE model that includes the explicit dispersion state of nanofillers and an interphase dielectric permittivity model inspired by viscoelasticity analysis in the frequency domain. We first present the constitutive model to capture the dielectric relaxation behavior for pure polymers in terms of a 'dielectric Prony Series', and illustrate the interphase property represented by shift factors. Then, to show that the proposed model can capture the influence of surface chemistry on composite behavior, we use experimental data from nanodielectrics of an epoxy matrix with functionalized nano-sized silica fillers as an example system. The system includes explicit microstructure morphology as input with advanced image processing techniques. With this model, we then perform parametric studies to look at the effect of interphase as well as the influence of microstructure dispersion on bulk composite dielectric response.

2 MATERIALS AND METHODS

An FE model is developed with a commercial software package (COMSOL) to simulate the dielectric spectroscopy data of polymer composites. Explicit morphology of nanodielectrics samples, i.e., experimentally determined dispersion of the nanosilica fillers in an epoxy matrix, is used as input to the FE model. Properties of silica fillers are obtained from literature, while bulk neat epoxy properties are measured from experiment. Properties of the interphase are obtained through an iterative tuning procedure by comparing the output from the FE model to experimental data until a good match is reached. The outcome of the FE model is the dielectric spectroscopy of the nanodielectric composite calculated at each frequency with dielectric constant and loss. During the tuning process, a set of optimal parameters that define the permittivity deviation of the interphase from the pure polymer can also be obtained.

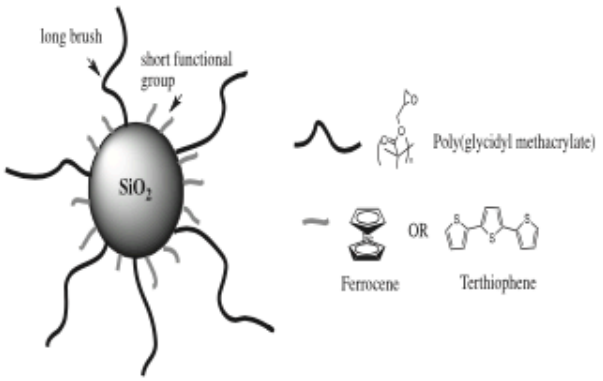

Figure 1. Sample material systems used in this FEA model. Left: schematic showing bimodal grafts on silica nanoparticle. Right: long (PGMA) and small (ferrocene or terthiophine) chains of grafts.

2.1 EXPERIMENTAL DATA

Detail about experimental samples is described in our previous work [8]. It shows that the use of two populations of molecules (a bimodal brush – see Figure 1) on a nanosilica particle surface can be used to improve filler dispersion and breakdown strength (up to 40 %). In this case, a high graft density of short molecules that have potential electron or hole trapping states - such as ferrocene and terthiophene, and a low graft density of matrix compatible long molecules poly(glycidyl methacrylate) (PGMA) were used. It has been observed that bimodal brush functionalized epoxy nanodielectrics exhibit dielectric properties that depend on the surface chemistry of the silica nanoparticle. FEA modeling in this work was implemented based on experimental data from tunneling electron microscopy (TEM) images (Figure 2) and dielectric spectra (Figure 3). The increase in dielectric loss at low frequency observed in both the neat polymer and composites is due to the alpha relaxation caused by polymer backbone chain motion. The peak around 10^4 Hz is due to beta relaxation caused by side chain crankshaft motion. The difference among dispersion states as observed in Figure 2 is due to the subtle changes in the long chain graft density and length as well as the enthalpic incompatibility of the short molecule with the matrix, which changes the interface thermodynamics and thus dispersion. To simulate any potential interfacial polarization, the DC conductivity of the matrix and interfacial region was set to 10^{-15} S/m.

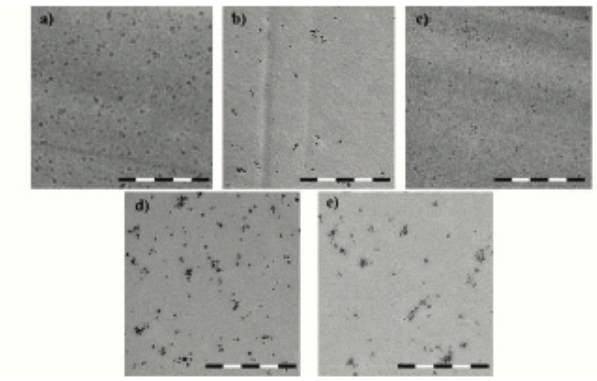

Figure 2. TEM images of bimodal brush functionalized epoxy nanocomposite. (a) bimodal anthracene, (b) biomodal ferrocene, (c) bimodal monothiphene, (d) monomodal PGMA, (e) bimodal terthiophene. All scale bars are 500 nm.

2.2 CONSTITUTIVE MODEL

With relaxation of a single element represented as a standard Debye function, a formulation of dielectric relaxation in a polymer can be obtained per similarity between the viscoelastic Prony Series and Debye relaxation expressions. Through detailed derivations shown in the Appendix, a 'dielectric Prony Series' can be expressed as

$$\begin{cases} \varepsilon'(\omega) = \varepsilon_\infty + \sum_{i=1}^{n} \dfrac{\Delta\varepsilon_i}{1+(\omega\tau_i)^2} \\ \varepsilon''(\omega) = \sum_{i=1}^{n} \dfrac{\Delta\varepsilon_i \omega\tau_i}{1+(\omega\tau_i)^2} \end{cases} \quad (1)$$

where ε' and ε'' are the real and imaginary parts of dielectric permittivity as a function of the angular frequency, ω; τ_i is the relaxation time; ε_∞ is the real permittivity at high frequency; $\Delta\varepsilon_i$ is the dielectric relaxation strength or intensity as the difference between permittivity at a given frequency and ε_∞. This formulation enables fast calibration of the polymer matrix properties using an established algorithm [21], and can be used to investigate dielectric relaxation behavior of the neat polymer matrix and interphase.

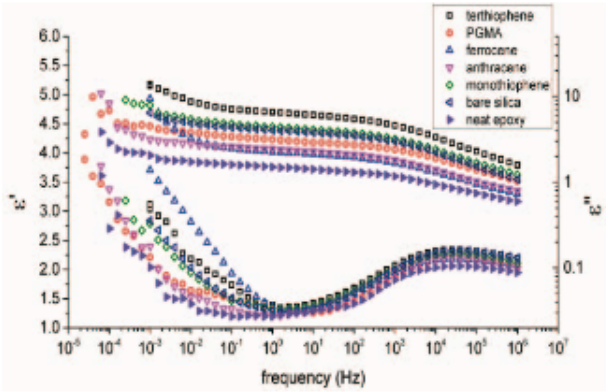

Figure 3. Experimental data of permittivity of the nanodielectric samples at room temperature. Neat epoxy: pure polymer matrix. Bare silica: polymer nanocomposite containing fillers without surface treatment. PGMA: nanocomposite with monomodal PGMA long chains. The other samples contain nanofillers grafted with bimodal PGMA and corresponding short chains. All composite samples have 2 wt% loading of fillers.

2.3 FINITE ELEMENT MODEL

A two-dimensional electric current model in the frequency domain is set up in COMSOL. A schematic of the FE framework workflow with boundary conditions and sample geometry is shown in Figure 4. To simulate the composite as a representative volume element (RVE), a square with side length of one micrometer is used as the simulation domain. As nanosilica fillers have an average diameter of 15 nm [22], this domain size ensures a representative state of filler dispersion and clustering. From the original TEM image in Figure 4a, a binary image showing the nanofiller and matrix phases as in Figure 4b is generated using a previously developed image analysis algorithm [22], which eliminates the effect of uneven background brightness and noisy points. Our model takes aggregation of spherical nanoparticles as visually identifiable clusters from the micrograph. The clusters are represented as ellipses as shown in Figure 4c. Geometry of the ellipses, including major and minor axes, orientation, and positions, are also identified from image processing. It is assumed that interfacial region associated with different nanofillers (outline of interphase shown as surrounding ellipses in Figure 4c) can overlap when the nanofillers are close to each other. The model is then configured with a given loading, which is represented as the volume fraction (VF) of fillers in the composite. To ensure the final VF used in FE is the same as in original sample, major and minor axes of cluster ellipses are scaled accordingly so that the total area percentage of clusters is equal to the labeled

VF of the experimental sample. Triangular elements are then used to mesh the microstructure with a finer mesh in the interphase area to capture the details of geometric features as well as local interphase property. Periodic boundary conditions are applied on lateral surfaces. AC voltage is applied at the bottom of the domain with the top surface grounded so that the configuration resembles a parallel plate capacitor.

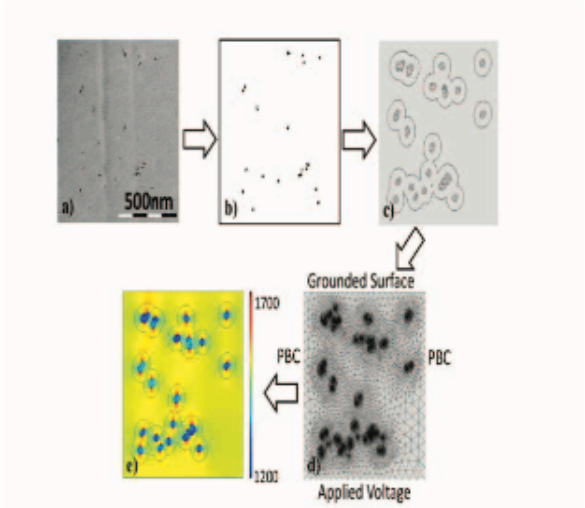

Figure 4. Configuration of FE model geometry in COMSOL. a) original TEM micrograph from experiment, b) binary image of filler (black) and matrix (white) phases, c) geometry used in FE after image processing with short molecules and interphase shown as outlines around fillers that correspond to bimodal grafts, d) FE configuration showing mesh with triangular elements and boundary conditions (PBC stands for periodic boundary condition), e) result from FE showing electric field intensity distribution with explicit inclusion of interphase (unit in V/m). Sample shown: bimodal ferrocene-PGMA grafted silica in epoxy

As shown in Figure 5a, the region between filler and matrix is represented by a two-phase configuration with a thin layer of small functional molecules surrounded by a more extensive layer of interphase. The thickness of this thin layer is taken as 10 nm in the FE model to represent the impact of bimodal chain grafts near the nanofiller surface. Based on previous studies on filler-filler spacing and interphase in nanodielectrics [2, 3], a reasonable thickness of the interphase is assumed to be 50 nm. Relative permittivity of silica fillers and small functional molecules are taken from the literature with values shown in Table 1 [23-26]. Electric conductivity for the neat polymer is assumed to be very small and bearing the same value as the silica filler with a constant value of 10^{-15} S/m. For the polymer matrix, the relative permittivity is represented as a frequency dependent complex function covering a wide frequency range from 10^{-3} Hz to 10^{6} Hz, which includes dipolar, ionic and electronic components, as represented by the Prony Series in Equation (1). The interphase is expressed with a similar Prony Series formulation with additional shift terms, which will be shown in Section 3.3. With geometry and material input property configured for all phases as shown in Figure 5b, FE analysis is then performed to obtain current density distribution, which can be used to derive bulk dielectric permittivity in the nanodielectric composite using

$$\varepsilon_r(\omega) = \frac{j_y^*(\omega)d}{j\omega V^*(\omega)\varepsilon_0} - \frac{\sigma_0 j}{\varepsilon_0 \omega} \qquad (2)$$

where $V^*(\omega)$ is the applied voltage as a function of angular frequency ω, and $j_y^*(\omega)$ is the component of the average complex AC current density perpendicular to the grounded surface. d is the side length of simulation domain, and ε_0 is the vacuum permittivity of 8.85×10^{-12} F/m.

Table 1. Dielectric Permittivity of Small Functional Molecules and Filler for Samples used in this Model.

Component	ε'	ε''
silica	3.9	0
thiophene	2.4	0.001
ferrocene	4	0.24
anthracene	3.1	0.05

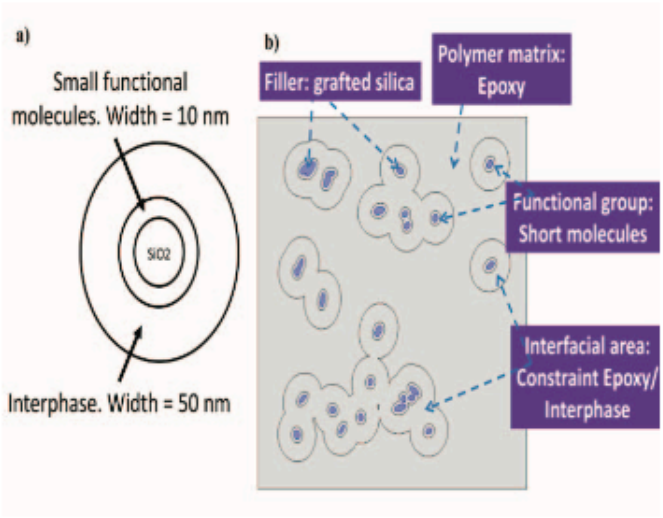

Figure 5. Configuration of material phases in the FE model. a) schematic of a single spherical grafted filler with two layers, b) four phases of constituents used in FE model. The irregular shapes of cluster are aggregation of multiple spherical fillers.

3 RESULTS AND DISCUSSION

Dielectric spectroscopy for the polymer matrix and the composites can then be analyzed using Equation 1 and the developed FE model. In this section, the procedure for obtaining the Prony Series coefficients for the pure polymer is first discussed, followed by a formulation of interphase properties represented as shifted property from the pure polymer. Examples of shift factor derivation for several nanodielectric systems are then demonstrated as case studies. Lastly, the influence of interphase thickness and dispersion is detailed to show the critical effect of the inclusion of interphase in this FE framework.

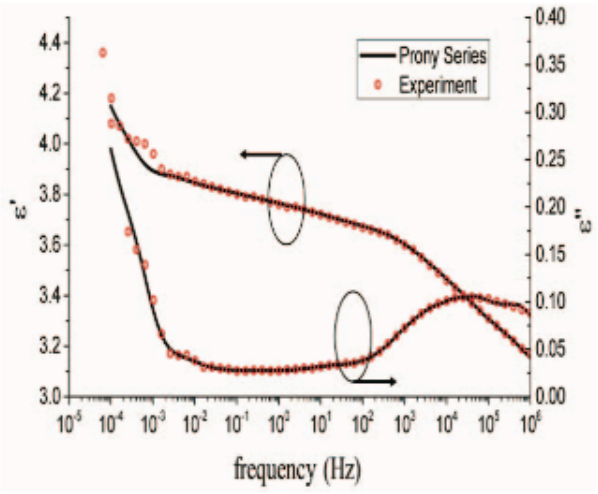

Figure 6. Comparison of real and imaginary permittivity of epoxy matrix with Prony Series and experimental data.

3.1 PURE POLYMER MATRIX

The dielectric Prony Series can capture broadened and shifted relaxation behaviors in neat epoxy at room temperature. Using Equation (1) with n = 25, the relaxation spectra of epoxy can be accurately captured as shown in Figure 6. It is observed that the relaxation peaks of epoxy at both low and high frequency are well captured by the Prony Series, which demonstrates the Prony Series formulation as a valid approach to describe polymer dielectric relaxation. The Prony Series coefficients fitted from Equation (1) are thus used to represent the properties of the pure polymer.

3.2 INFLUENCE OF SMALL MOLECULES

Experimental data has revealed that small functional molecules on the nanofiller surface can trap charges and lower the charge mobility, which may decrease the effective conductivity although the local conductivity may increase [27]. Since the length scale of the space that the small molecules occupy is below the Debye length, the conductivity effect of the small functional molecules can thus be neglected in this FE model. For dielectric permittivity, the small functional molecules possess a different dielectric constant from the neat polymer and filler. In this FE model, the macroscopic dielectric constant of the small molecules in a pure solid is assumed for the local properties as shown in Table 1.

3.3 INTERHASE MODEL

One of the core features in this FE model is the configuration of the filler-matrix interphase, which lies adjacent to the dense small functional molecules and extends into the pure polymer. Dielectric permittivity of the interfacial polymer is modeled by the Prony Series expression with additional parameters:

$$\varepsilon_{\text{int}}'(\omega) = \varepsilon_{\infty} + c + M_{\alpha}\sum_{\tau_i>\tau_0}\frac{\Delta\varepsilon_i}{1+\left(\omega S_{\alpha}\tau_i\right)^2} + M_{\beta}\sum_{\tau_i<\tau_0}\frac{\Delta\varepsilon_i}{1+\left(\omega S_{\beta}\tau_i\right)^2} \quad (3)$$

$$\varepsilon_{\text{int}}''(\omega) = M_{\alpha}\sum_{\tau_i>\tau_0}\frac{\omega S_{\alpha}\tau_i\Delta\varepsilon_i}{1+\left(\omega S_{\alpha}\tau_i\right)^2} + M_{\beta}\sum_{\tau_i<\tau_0}\frac{\omega S_{\beta}\tau_i\Delta\varepsilon_i}{1+\left(\omega S_{\beta}\tau_i\right)^2} \quad (4)$$

In this interphase model, the alpha and beta relaxations are modeled separately. Based on experimental results, the threshold value of the relaxation time, τ_0, is chosen so that the corresponding threshold frequency, $\omega_0 = 1/(2\pi\tau_0)$, separates the relaxation peak into low and high frequency regions. Elements with τ_i greater than τ_0 are modeled as alpha (low frequency) relaxation while those with τ_i smaller than τ_0 are modeled as beta relaxation (high frequency). M_α and M_β account for change of intensity for respective relaxations, shifting the permittivity curve vertically. S_α and S_β characterize the shift of relaxation times and move the curve in a horizontal direction. An additional constant, c, describes the change in ε_∞ in the interphase.

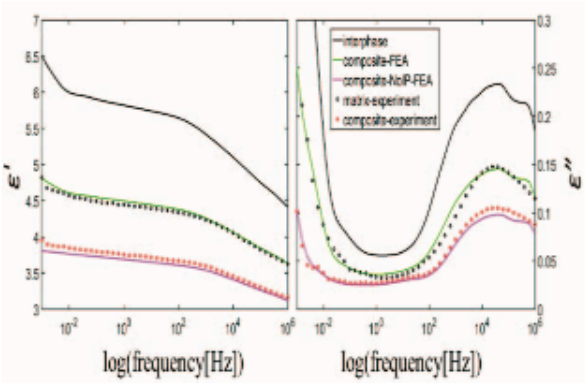

Figure 7. Comparison between simulated dielectric spectra and experimental data for 2 wt% bimodal monothiophene grafted silica in epoxy.

A similar iterative tuning process from our previous work [28] is adopted here to optimize values of tuning parameters. An example of a fitted result is shown in Figure 7 using data from monothiophene-PGMA bimodal sample. The results indicate that the configuration of the interfacial area is essential in the modeling. With the interphase deactivated (two-phase composite consisting of only polymer matrix and fillers, shown as composite-NoIP-FEA), the simulated permittivity is almost identical to the experimental data for the neat polymer. This result indicates that inclusion of the interphase is critical to accurately simulate composite permittivity. The local interphase property is also shown with a significant permittivity and loss enhancement to the neat matrix polymer. This change, we argue, is due to the presence of nanoparticles, which changes the mobility of the polymer chains around them and consequently results in the alternated dipole orientation at the interphase. Simulation result is improved by including the interphase as shown by composite-FEA, which includes all four material phases, including filler,

Table 2. Summary of Shift Factors for Bimodal Nanodielectric Systems with Different Surface Treatment.

Sample	τ_0	S_β	M_β	S_α	M_α	c
Bimodal monothiophene	0.01	1	2.2	0.1	2	1.2
Bimodal anthracene	0.1	0.9	1.55	0.2	0.7	0.3
Bimodal terthiophene	0.1	1	3	5	2	2.5
Monomodal PGMA	0.01	0.4	1.55	0.01	1	1.5
Bimodal ferrocene	0.01	0.75	1.8	0.006	1.4	0.3

matrix, small functional molecules, and interphase. Through the tuning process, optimal parameters for the interphase can be obtained to achieve a good match to the experimental data.

We applied the same methodology to five silica-epoxy nanodielectric systems with different types of small molecule grafts. Results of the interphase are shown in Table 2. It can be observed that S is typically smaller than one while M is

larger than one (upward shift in nanocomposite from polymer baseline), indicating higher chain mobility because of additional grafted nanoparticles. This agrees with the experimental data where the addition of grafts on fillers enhances the relative permittivity. Exceptions occur for S_α for the terthiophene-PGMA sample, which has a value of 5. This exception is possibly due to the distinct interaction between the terthiophene and matrix polymer. In general, addition of short molecules caused a positive shift in relaxation. These results show that the variation in polarizability and chain mobility at the interphase caused by the chemistry of small functional molecules can be captured by the interphase parameters in this FE model.

The interfacial region as well as the dispersion state of the nanofillers both play a critical role to provide altered dielectric permittivity in the nanocomposite. Using the established FE framework, parametric analysis on the influence of interphase thickness and dispersion on composite dielectric permittivity can be performed. The first study varies interphase thickness while keeping the other model parameters constant. The second study iterates through filler dispersion with various degrees of cluster aggregation and dispersion.

3.4 INFLUENCE OF INTERPHASE THICKNESS

Here we use the developed FE model to investigate how the size of the interphase influences the composite properties. The interphase properties are fixed during this study, and shift factors are selected from Table 2 as used in Equations (3) and (4) for bimodal ferrocene-PGMA. The microstructure dispersion state is taken from processed TEM micrographs, and remains the same with identical filler position, size, and orientation for all cases. The thin layer of short molecules also remains unchanged with constant permittivity of $4 - 0.24j$ and conductivity of 10^{-15} S/m.

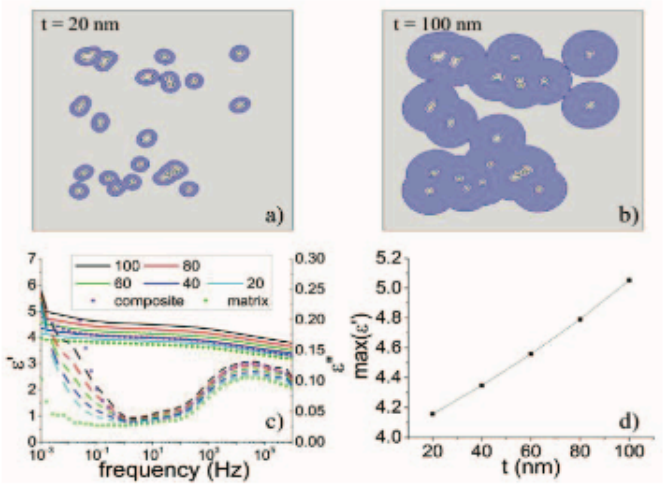

Figure 8. Parametric study on the influence of interphase thickness on dielectric permittivity of nanodielectric. Microstructure dispersion of bimodal ferrocene-PGMA sample with highlighted interphase thickness of a) 20 nm, and b) 100 nm; c) FE result of dielectric permittivity using different interphase thickness with comparison to experimental data of composite and matrix; d) maximum permittivity from FE simulation as a function of interphase thickness, t.

Figure 8 shows the permittivity for composites with different interphase thickness determined from FEA. The highlighted region in Figure 8a and Figure 8b shows the interphase region for the smallest and largest interphase thicknesses. Figure 8c shows results of permittivity for a range of tested interphase thicknesses. As M_α and M_β are both larger than one (which indicates more polarization for α and β relaxations at the interphase), both real and imaginary parts of permittivity increase with interphase across the entire frequency range. Figure 8d plots the maximum value of ε' for each case. For 5X increase in interphase thickness, max (ε') increases by 20%, which is a larger increase than the difference between composite permittivity of ferrocene-PGMA and neat polymer from the experiment. From this study, we can conclude: 1) for an interphase with enhanced properties compared to the neat polymer (with M_α and/or M_β larger than one), composite permittivity from simulation increases with the interphase thickness, and 2) the change of simulated composite property because of increasing interphase thickness can exceed the difference between experimental data of the composite and neat polymer. This result indicates that the interphase thickness is an important factor that determines composite dielectric performance.

3.5 INFLUENCE OF FILLER DISPERSION

Experimental data suggests that a well dispersed microstructure of nanofillers provides positive enhancements in composite material properties [27]. To analyze the influence of dispersion state, artificially reconstructed microstructures with different degrees of nanoparticle agglomeration are tested with the FE model. The dispersion geometries with various degrees of filler agglomeration are generated with a descriptor-based microstructure reconstruction algorithm previously developed and used for analysis of viscoelasticity in polymer

nanocomposites [16, 17, 19]. Given the five input parameters that specify statistical distribution of the fillers (volume fraction, domain size, equivalent radius, nearest neighbor distance, and aspect ratio), geometric configuration of fillers can be generated in terms of position, size (major and minor axes), and orientation angle. Figure 9a-d shows examples with different degrees of dispersion. For these simulations, the VF of fillers is maintained at 1 vol%. As the number of fillers, N, increases, the microstructure becomes more dispersed resulting in a larger total interphase area. These microstructures are then imported to the FE model and assigned with boundary conditions and material properties.

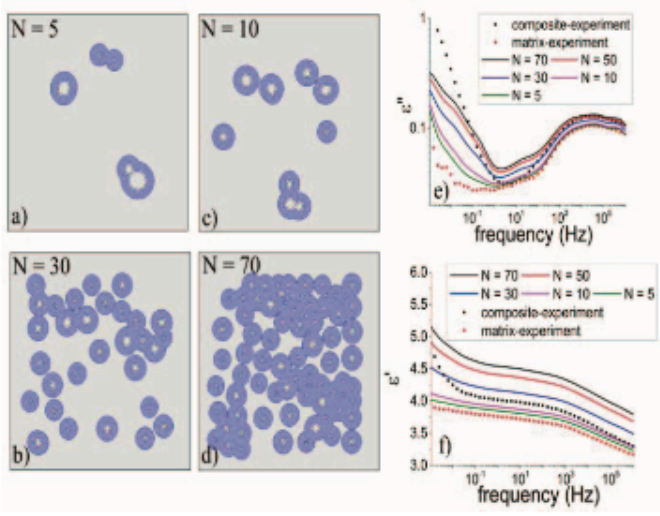

Figure 9. Comparison of dispersion states of microstructure using descriptor reconstruction and FEA results. Top: geometry of filler dispersion from FEA with total number of fillers, N. Highlighted area shows interphase; bottom: real and imaginary components permittivity from FEA result.

FE results from five dispersion states are compared with experimental data of matrix and composite in Figure 9e-f. Like the interphase parametric study, samples with larger total interphase area exhibit higher composite permittivity and loss. Result suggests that for the more dispersed cases with N of 30 or more, composite dielectric constant from FEA is higher than the experimental data, while for the more aggregated cases (N = 5 and 10), the simulated composite dielectric constant is smaller than experimental data. This result indicates that the dispersion state of the fillers can have a significant impact on the dielectric behavior. The case with the highest degree of dispersion (N=70) has been shown to result in more than 30% increase in dielectric constant compared with the case with the most aggregated fillers (N=5). A desired composite property can thus be tuned by controlling the dispersion state of fillers.

4 CONCLUSION

An FE framework using a dielectric permittivity model inspired from viscoelasticity constitutive equations has been demonstrated using bimodal grafted nanosilica in epoxy as a testbed. A superposition of standard Debye functions using multiple relaxation times is formulated, like a viscoelastic Prony Series, where coefficients from the superposition series can be calculated using an algorithm borrowed from viscoelastic analysis. Using the dielectric Prony Series constitutive relation, an FE model is developed to simulate dielectric permittivity in nanocomposites with input of explicit dispersion geometry and inclusion of filler-matrix interphase. The difference in properties of the interphase polymer from the neat polymer, arising from deviation of chain mobility at the interactive region between grafted nanoparticles and backbone chains, is addressed by shift factors applied to the Prony Series. Values of the shift factors were determined from an iterative optimization tuning process by matching simulated property from FE analysis with experimental data. Based on the results of interphase shift factors, the interphase area in our tested samples is likely to have an enhanced chain mobility and polarizability in the measured frequency range.

Using the developed model, the influence of interphase thickness and degree of agglomeration of fillers is investigated. Results from the parametric studies show that the simulated composite dielectric permittivity varies per total interphase area. Results demonstrate that for an interfacial region of stronger chain mobility, by increasing either interphase thickness or improving dispersion, a higher composite dielectric constant can be obtained.

The FE model can be a powerful tool to describe broadband dielectric spectroscopy behavior in nanocomposites. Through careful tuning and calibration with experimental data, it has the potential to provide insights into the physics of the interphase, especially under the influence of different surface chemistries, which is difficult for direct measurement through experiments. To assist with design of novel nanodielectric materials, additional studies can be performed to analyze the effect of different types and configurations of fillers, for example, elongated fillers with higher aspect ratios and anisotropic microstructure using advanced microstructure reconstruction techniques [29]. Although our simulations based on 2D model can successfully analyze and explain the effect of interphase, 3D FE analysis should be explored to correlate the physical configuration of material phases with experimental data. In addition, effect of conductivity of the small functional molecules as well as low frequency range of the dielectric loss needs to be taken into consideration in future work.

APPENDIX

A.1 DERIVATION OF DIELECTRIC PRONY SERIES

Three constitutive equations are considered in solving the dielectric response:

$$\vec{D}(r,t) = \varepsilon(r)\vec{E}(r,t) \quad \text{(A1)}$$

$$\frac{\partial \rho}{\partial t} + \nabla \bullet \vec{j} = 0 \quad \text{(A2)}$$

$$\vec{j} = \sigma \vec{E} + \frac{\partial \vec{D}}{\partial t} \quad \text{(A3)}$$

where D is electric displacement, ε is relative permittivity, E is electric field, ρ is charge density, j is current density, σ is

electric conductivity, with r and t as spatial and temporal independent variables, respectively.

For ε, an ideal relaxation with a single relaxation time is commonly expressed as a Debye function [15, 30],

$$\varepsilon^*(\omega) = \varepsilon_\infty + \frac{\Delta\varepsilon}{1+i\omega\tau} \tag{A4}$$

or equivalently dividing the complex expression into real and imaginary parts,

$$\begin{cases} \varepsilon'(\omega) = \varepsilon_\infty + \dfrac{\Delta\varepsilon}{1+(\omega\tau)^2} \\ \varepsilon''(\omega) = \dfrac{\Delta\varepsilon\omega\tau}{1+(\omega\tau)^2} \end{cases} \tag{A5}$$

where $\varepsilon^*(\omega)$ is the complex dielectric permittivity as a function of the angular frequency ω and ε' and ε'' are the real and imaginary parts, respectively ($\varepsilon^* = \varepsilon' + i\varepsilon''$); ε_∞ is the real permittivity at high frequency; τ is the relaxation time and $\Delta\varepsilon$ is the dielectric relaxation strength or intensity as the difference between instantaneous permittivity and ε_∞.

In viscoelasticity theory, the dynamic mechanical response of storage and loss moduli can be represented by the frequency-domain Prony Series [18]:

$$\begin{cases} E'(\omega) = E_\infty + \sum_{i=1}^{n} \dfrac{E_i(\omega\tau_i)^2}{1+(\omega\tau_i)^2} \\ E''(\omega) = \sum_{i=1}^{n} \dfrac{E_i\omega\tau_i}{1+(\omega\tau_i)^2} \end{cases} \tag{A6}$$

where E' and E'' are the real and imaginary part of the dynamic moduli (storage and loss moduli, respectively); E_∞ is the equilibrium modulus once the material is fully relaxed; τ_i is the relaxation time; E_i is the elastic modulus of each element in the generalized Maxwell model. Here, E_i and τ_i are Prony Series coefficients, which can be obtained from experimental data of complex modulus using a previously developed algorithm [21]. This algorithm allows simultaneous fitting of real and imaginary parts of the superposition expression as in Equation A6.

Relaxation behavior in dielectrics can be compared with viscoelastic relaxation under linear response theory with dielectric permittivity as the generalized compliance [31]. We observe similarity between each element in the viscoelastic Prony Series and the standard dielectric Debye function, where the denominator and numerator for the imaginary part of both properties shares the same expression. Therefore, similarly to the viscoelastic Prony Series, we propose to represent the dielectric relaxation behavior in polymers as a superposition of characteristic relaxations represented by multiple Debye elements with different relaxation times. We express the 'dielectric Prony Series' in the following form:

$$\begin{cases} \varepsilon'(\omega) = \varepsilon_\infty + \sum_{i=1}^{n} \dfrac{\Delta\varepsilon_i}{1+(\omega\tau_i)^2} \\ \varepsilon''(\omega) = \sum_{i=1}^{n} \dfrac{\Delta\varepsilon_i\omega\tau_i}{1+(\omega\tau_i)^2} \end{cases} \tag{A7}$$

It is noted that the only difference between expressions of viscoelastic and dielectric Prony Series is the numerator of the real part. We aim to follow a similar approach to obtaining Prony Series coefficients in dielectrics using an algorithm previously developed for fast approximation of Prony Series coefficients, and a simple modification to the expression is needed in order to apply the same algorithm on dielectric data.

Consider the real permittivity at $\omega = 0$ Hz (we denote $\varepsilon_0 = \varepsilon'(\omega = 0)$ thereafter),

$$\varepsilon_0 = \varepsilon_\infty + \sum_{i=1}^{n} \Delta\varepsilon_i \tag{A8}$$

Subtracting $\varepsilon'(\omega)$ from $\varepsilon'_0 + \varepsilon_\infty$ and re-arranging the terms, one obtains

$$\varepsilon'_0 + \varepsilon_\infty - \varepsilon'(\omega) = \varepsilon_\infty + \sum_{i=1}^{n} \frac{\Delta\varepsilon_i(\omega\tau_i)^2}{1+(\omega\tau_i)^2} \tag{A9}$$

The right-hand side of Equation (A9) is now the same as the expression for storage modulus as in Equation (A6). In practice, ε_∞ and ε'_0 are approximated as the relative permittivity at the highest and lowest frequency from experimental testing. Thus, with measured complex dielectric spectroscopy data of the pure polymer material, $\varepsilon^*(\omega)$, dielectric strength, $\Delta\varepsilon_i$, and relaxation time constant, τ_i, can be obtained as the Prony Series coefficients, which can be used to investigate dielectric relaxation behavior of the neat polymer matrix and interphase.

ACKNOWLEDGMENT

The authors acknowledge Office of Naval Research (Grant N000141310173) and National Science Foundation (CMMI-1334929, 1333977, 1310292) for partial support of this work. The authors thank Prof. Curt Breneman and Dr. Ke Wu for useful discussions.

REFERENCES

[1] J. K. Nelson, *Dielectric Polymer Nanocomposites,* New York: Springer, 2010.

[2] J. K. Nelson, "Overview of nanodielectrics: Insulating materials of the future," IEEE Electr. Insul. Conf. and Electr. Manuf. Expo., pp. 229-235, 2007

[3] T. Tanaka, M. Kozako, N. Fuse, and Y. Ohki, "Proposal of a multi-core model for polymer nanocomposite dielectrics," IEEE Trans. Dielectr. Electr. Insul., Vol. 12, No. 4, pp. 669-681, 2005.

[4] M. Roy, J. Nelson, R. MacCrone, L. S. Schadler, C. Reed, and R. Keefe, "Polymer nanocomposite dielectrics-the role of the interface," IEEE Trans. Dielectr. Electr. Insul., Vol. 12, No. 4, pp. 629-643, 2005.

[5] A. P. Holt, P. J. Griffin, V. Bocharova, A. L. Agapov, A. E. Imel, M. D. Dadmun, J. R. Sangoro, and A. P. Sokolov, "Dynamics at the polymer/nanoparticle interface in poly (2-vinylpyridine)/silica nanocomposites," Macromolecules, Vol. 47, No. 5, pp. 1837-1843, 2014.

[6] J. Mijovic, H. Lee, J. Kenny, and J. Mays, "Dynamics in polymer-silicate nanocomposites as studied by dielectric relaxation spectroscopy and dynamic mechanical spectroscopy," Macromolecules, Vol. 39, No. 6, pp. 2172-2182, 2006.

[7] B. Natarajan, T. Neely, A. Rungta, B. C. Benicewicz, and L. S. Schadler, "Thermomechanical properties of bimodal brush modified nanoparticle composites," Macromolecules, Vol. 46, No. 12, pp. 4909-4918, 2013.

[8] S. Virtanen, T. M. Krentz, J. K. Nelson, L. S. Schadler, M. Bell, B. Benicewicz, H. Hillborg, and S. Zhao, "Dielectric breakdown strength of epoxy bimodal-polymer-brush-grafted core functionalized silica nanocomposites," IEEE Trans. Dielectr. Electr. Insul., Vol. 21, No. 2, pp. 563-570, 2014.

[9] J. M. Garnett, " Garnett, J. M. (1905). Colours in Metal Glasses, in Metallic Films and in Metallic Solutions II," Proc. of the Roy. Soc. of London. Series A, Vol. 53, pp. 370-373, 1905.

[10] D. Bruggeman, "Calculation of various physics constants in heterogenous substances I Dielectricity constants and conductivity of mixed bodies from isotropic substances," Ann. Phys., Vol. 24, No. 7, pp. 636-664, 1935.

[11] K. Lichtenecker, "Dielectric constant of natural and synthetic mixtures," Phys. Z, Vol. 27, pp. 115-115, 1926.

[12] Z. Hashin, and S. Shtrikman, "A variational approach to the theory of the elastic behaviour of multiphase materials," J. Mechanics and Phys. Solids, Vol. 11, No. 2, pp. 127-140, 1963.

[13] M. G. Todd, and F. G. Shi, "Validation of a novel dielectric constant simulation model and the determination of its physical parameters," Microelectronics J., Vol. 33, No. 8, pp. 627-632, 2002.

[14] H. T. Vo, and F. G. Shi, "Towards model-based engineering of optoelectronic packaging materials: Dielectric constant modeling," Microelectronics J., Vol. 33, No. 5, pp. 409-415, 2002.

[15] A. Schönhals, and F. Kremer, Analysis of Dielectric Spectra, Broadband Dielectric Spectroscopy, pp. 59-98: Springer, 2003.

[16] B. Natarajan, Y. Li, H. Deng, L. C. Brinson, and L. S. Schadler, "Effect of interfacial energetics on dispersion and glass transition temperature in polymer nanocomposites," Macromolecules, Vol. 46, No. 7, pp. 2833-2841, 2013.

[17] H. Xu, Y. Li, C. Brinson, and W. Chen, "A Descriptor-Based Design Methodology for Developing Heterogeneous Microstructural Materials System," J. Mechanical Design, Vol. 136, No. 5, pp. 051007, 2014.

[18] H. F. Brinson, and L. C. Brinson, Polymer Engineering Science and Viscoelasticity: Springer, 2008.

[19] C. M. Breneman, L. C. Brinson, L. S. Schadler, B. Natarajan, M. Krein, K. Wu, L. Morkowchuk, Y. Li, H. Deng, and H. Xu, "Stalking the Materials Genome: A Data-Driven Approach to the Virtual Design of Nanostructured Polymers," Advanced Functional Materials, Vol. 23, No. 46, pp. 5746-5752, 2013.

[20] I. Preda, J. Castellon, M. Frechette, and S. Agnel, "Modelling the dielectric permittivity of nanocomposites-the overlap model." IEEE Proc. Int'l. Symp. Elec. Insul. Mat. pp. 17-21, 2014

[21] R. D. Bradshaw, and L. Brinson, "A sign control method for fitting and interconverting material functions for linearly viscoelastic solids," Mechanics of Time-Dependent Materials, Vol. 1, No. 1, pp. 85-108, 1997.

[22] I. Hassinger, X. Li, H. Zhao, H. Xu, Y. Huang, A. Prasad, L. Schadler, W. Chen, and L. C. Brinson, "Toward the development of a quantitative tool for predicting dispersion of nanocomposites under non-equilibrium processing conditions," J. Materials Sci., Vol. 51, No. 9, pp. 1-12, 2016

[23] J. Han, H. Xu, Z. Zhu, X. Yu, and W. Li, "Terahertz spectroscopy of naphthalene, α-naphthol, β-naphthol, biphenyl and anthracene," Chem. Phys. Letters, Vol. 392, No. 4, pp. 348-351, 2004.

[24] S. D. Phadke, "Dielectric properties of plasma-polymerized ferrocene films," Thin Solid Films, Vol. 48, No. 3, pp. 319-324, 1978.

[25] J.-J. Pinvidic, S. Takahara, O. Yamamuro, and H. Suga, "Dielectric study of crystalline thiophene," Solid state communications, Vol. 72, No. 5, pp. 501-505, 1989.

[26] P. R. Gray, P. Hurst, R. G. Meyer, and S. Lewis, *Analysis and Design of Analog Integrated Circuits*, Wiley, 2001.

[27] T. M. Krentz, Y. Huang, J. K. Nelson, L. S. Schadler, M. Bell, B. Benicewicz, S. Zhao, and H. Hillborg, "Enhanced charge trapping in bimodal brush functionalized silica-epoxy nanocomposite dielectrics." IEEE Conf. Electr. Insul. Dielectr. Phenomena, pp. 643-646.

[28] Y. Huang, T. M. Krentz, J. K. Nelson, L. S. Schadler, Y. Li, H. Zhao, L. C. Brinson, M. Bell, B. Benicewicz, and K. Wu, "Prediction of interface dielectric relaxations in bimodal brush functionalized epoxy nanodielectrics by finite element analysis method," IEEE Conf. Electr. Insul. Dielectr. Phenomena, pp. 748-751, 2014

[29] Y. Zhang, H. Zhao, I. Hassinger, L. C. Brinson, L. S. Schadler, and W. Chen, "Microstructure reconstruction and structural equation modeling for computational design of nanodielectrics," Integrating Materials and Manufacturing Innovation, Vol. 4, No. 1, pp. 1-26, 2015.

[30] P. J. W. Debye, *Polar Molecules*: Chemical Catalog Company, Incorporated, 1929.

[31] T. Pakula, *Dielectric and Mechanical Spectroscopy—a Comparison, Broadband Dielectric Spectroscopy*, pp. 597-623, Springer, 2003.

He Zhao received his B.S. degree from the University of Notre Dame in 2012. He has been a Ph.D. student with Prof. L. Catherine Brinson at Northwestern University since 2012. His research focuses on modeling of polymer nanocomposites and nanodielectrics with finite element and data-driven methods.

Yang Li received his B.S. degree from Shanghai Jiao Tong University in 2009 and his Ph.D. degree from Northwestern University in 2014. He joined Research and Innovation Center at Ford Motor Company as a research engineer in composites manufacturing in 2014. His current research focus is simulation of manufacturing process of carbon fiber composites for automotive applications. He received Ford Motor Company Global CAE Innovation Chief Award in 2015.

L. Catherine Brinson received her B.S. degree from Virginia Tech and Ph.D. degree from Caltech in Applied Mechanics. She joined the Northwestern faculty in 1992 and is currently the Jerome B. Cohen Professor of Mechanical Engineering. She also holds faculty position in the Materials Science and Engineering department at Northwestern, and serves as Associate Dean at the McCormick School of Engineering. She is fellows of ASME and SES. Her research interests focus on studies of advanced nanomaterials and polymer nanocomposites.

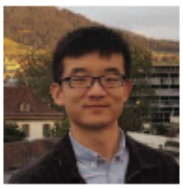

Yanhui Huang received his B.Sc. degree from Shanghai Jiao Tong University in 2013 and Ph.D. degree in 2016 from Rensselaer Polytechnic Institute. His research involves both experiment test and computer modeling on nanodieletrics, with a special focus on charge transport and breakdown.

Timothy M. Krentz was born in Bethlehem, Pennsylvania in 1989. He received his B.S. degree from Lehigh University in 2011 and Ph.D. in 2016 from Rensselaer Polytechnic Institute. His research focuses on polymer nanocomposite dielectrics.

Linda S. Schadler received her B.S. degree from Cornell University and the Ph.D. degree from the University of Pennsylvania in Materials Science and Engineering. She is currently a Professor of Materials Science and Engineering at Rensselaer Polytechnic Institute. Before coming to Rensselaer in 1996, she was on the faculty at Drexel University and spent 2 years at IBM's T.J. Watson Research Center. She is a Fellow of ASM International and currently and ASM Board of Trustees Member.

Michael Bell was born in Salem, New Jersey in 1983. He received his B.S. degree in chemistry from the Richard Stockton College of New Jersey in 2009. After graduating, he interned at the Department of Homeland Security's, Transportation Security Laboratory, investigating trace explosive residues. He also gained industrial experience at Coim USA inc., a polymer production facility, where he worked within both quality control and research and development. In 2011 Michael joined the Benicewicz group at the University of South Carolina where his research focuses on using controlled radical polymerization techniques to synthesize dielectric polymer nanocomposites.

Brian C. Benicewicz received his B.S. degree from Florida Institute of Technology in 1976 and his Ph.D. degree in polymer chemistry from the University of Connecticut. He is currently Educational Foundation Distinguished Professor in the Department of Chemistry and Biochemistry, and holds the CoEE (Center of Economic Excellence) chair in polymer nanocomposite research at the University of South Carolina. Prior to his appointment at the University of South Carolina, he held positions at Celanese Research Company, Ethicon Inc. and Los Alamos National Laboratory and was a professor of chemistry and the director for the NYS Center for Polymer Synthesis at RPI. He has been the recipient of multiple awards including the LANL Distinguished Patent Award, the LANL "Excellence in Industrial Partnerships Award", the NASA Technical Achievement Award, and NASA Technology Program Award.